Published in final edited form as:
J Neurosci Res. 2013 December ; 91(12): 1639–1650. doi:10.1002/jnr.23287.

Characterization of Intercostal Muscle Pathology in Canine Degenerative Myelopathy: A Disease Model for Amyotrophic Lateral Sclerosis

Brandie R. Morgan[1], **Joan R. Coates**[3], **Gayle C. Johnson**[4], **Alyssa C. Bujnak**[1], and **Martin L. Katz**[2,*]

[1]Division of Biological Sciences, University of Missouri School of Medicine, Columbia, Missouri, USA 65211

[2]Mason Eye Institute, University of Missouri School of Medicine, Columbia, Missouri, USA 65212

[3]Department of Veterinary Medicine and Surgery, University of Missouri College of Veterinary Medicine, Columbia, Missouri, USA 65211

[4]Department of Veterinary Pathobiology, University of Missouri College of Veterinary Medicine, Columbia, Missouri, USA 65211

Abstract

Dogs homozygous for missense mutations in the *SOD1* gene develop a late-onset neuromuscular disorder called degenerative myelopathy (DM) that has many similarities to amyotrophic lateral sclerosis (ALS). Both disorders are characterized by widespread progressive declines in motor functions accompanied by atrophic changes in the descending spinal cord tracts , and some forms of ALS are also associated with *SOD1* mutations. In end-stage ALS, death usually occurs as a result of respiratory failure due to severe functional impairment of respiratory muscles. The mechanisms that lead to this loss of function are not known. Dogs with DM are euthanized at all stages of disease progression providing an opportunity to characterize the onset and progression of any pathological changes in the respiratory muscles that may precede respiratory failure. To characterize such potential disease-related pathology we evaluated intercostal muscles from Boxer and Pembroke Welsh Corgi dogs that were euthanized at various stages of DM disease progression. DM was found to result in intercostal muscle atrophy, fibrosis, increased variability in muscle fiber size and shape, and an alteration in muscle fiber type composition. This pathology was not accompanied by retraction of the motor neuron terminals from the muscle acetylcholine receptor complexes, suggesting that the muscle atrophy did not result from physical denervation. These findings provide a better understanding of the mechanisms that likely lead to respiratory failure in at least some forms of ALS and will be useful in the development and evaluation of potential therapeutic interventions using the DM model.

[*]Corresponding author at: Martin L. Katz University of Missouri School of Medicine Mason Eye Institute One Hospital Drive Columbia, Missouri, 65212, USA katzm@health.missouri.edu (M. Katz).

Keywords

Neurodegeneration; dog; *SOD1*; disease model; morphometry

INTRODUCTION

Canine degenerative myelopathy (DM) is an adult onset neurodegenerative disease characterized by progressive impairment of motor functions (Averill 1973). Initial clinical signs are seen in dogs 8 years or older and include loss of coordination and asymmetric, spastic weakness in the pelvic limbs, which progress to paraplegia within 1 year from clinical onset. If dogs are not euthanized in early disease stages, signs will progress to include flaccid tetraplegia, widespread muscle atrophy and difficulty swallowing (Coates et al. 2007; Coates and Wininger 2010). Dog owners often elect euthanasia when their dogs become paraplegic (Coates and Wininger 2010), but some are not euthanized until more advanced stages of the disease are reached.

DM has many similarities to some forms of human amyotrophic lateral sclerosis (ALS). Like DM, ALS is also a late adult onset neurodegenerative disorder characterized by progressive loss of motor functions (Andersen et al. 1996; Charcot J-M 1869). Although causes of most ALS cases are unknown, some sporadic and familial forms have been associated with mutations in superoxide dismutase-1 (*SOD1*), which encodes cytosolic Cu/Zn superoxide dismutase (Rosen et al. 1993). In 2009, we reported that dogs of multiple breeds with a confirmed diagnosis of DM were homozygous for the A allele of a *SOD1* missense mutation, *SOD1:c.118G>A*, which predicts p.E40K substitution in SOD1 (Awano et al. 2009). Based on clinical signs, genetic testing, and spinal cord histopathology, DM has been found to occur in many breeds, and is especially prevalent in Boxers and Pembroke Welsh Corgis (PWCs) (Coates and Wininger 2010). Despite growing knowledge of genetic associations in ALS, the underlying mechanisms and resulting pathology are still not well understood for either the human or canine disease (Al-Chalabi et al. 2012; Coates and Wininger 2010). A major impediment to elucidating mechanisms underlying disease pathology in ALS is the scarcity of tissues available for study. Tissues that are available from ALS patients are usually obtained postmortem at end-stage disease. Thus, pathologic descriptions of disease progression in ALS patients are few (Fischer et al. 2004). With DM, on the other hand, dogs are euthanized at various disease stages so tissues can be obtained to evaluate progression of disease pathology.

For many years DM was thought to be a disease that involved primarily the ascending and descending tracts of the spinal cord and not the peripheral nervous system (Averill 1973; Griffiths and Duncan 1975). At disease onset, spinal reflexes are consistent with upper motor neuron (UMN) loss. Spinal cord pathology is most evident in the thoracic spinal cord early in the disease, spreads cranially and caudally, and becomes more severe as the disease progresses (Averill 1973; March et al. 2009). More recently, clinical descriptions and histopathology indicate that DM reaches beyond the spinal cord to also involve motor units, at least in the advanced stages of disease (motor neuron, axon, and myofiber) (Awano et al. 2009; Shelton et al. 2012). The distribution of lesions and clinical disease progression in

DM are similar to that reported for the UMN-onset ALS, with UMN signs in DM-affected dogs progressing to lower motor neuron (LMN) signs (Brooks et al. 2000; Coates et al. 2007; Coates and Wininger 2010).

To further assess DM as a potential disease model of ALS, studies were conducted to evaluate a thoracic motor unit in DM-affected dogs. We selected this site because the pathology in the ascending and descending tracts begins in the thoracic region of the spinal cord and because it was anticipated that tissue samples could be obtained from this region that represent all stages of DM disease progression. Thoracic motor units become impaired in ALS causing failure of respiratory muscles (de Carvalho et al. 2010), so evaluation of pathology in this region in DM is likely to be relevant to at least some forms of ALS.

MATERIALS AND METHODS

Tissue collections and disease status determinations

Tissues were obtained from companion dogs between 2009 and 2013. Tissues were acquired from 9 Boxers (4 control ages 8 to13 years; and 5 DM-affected ages 9 to 12 years) and 20 Pembroke Welsh Corgis (PWCs) (6 control, age's 12 to17 years; and 14 DM-affected, age's 12 to15 years). Sample collection protocols were approved by the University of Missouri Animal Care and Use Committee. Dogs with a presumptive diagnosis of DM, based on clinical signs of progressive upper motor neuron paresis and general proprioceptive ataxia of the pelvic limbs (Coates and Wininger 2010), were referred to various academic, private specialty or general practices. Dogs were excluded if their clinical signs were associated with spinal cord compressive lesions detected by magnetic resonance imaging or myelography or if the dog exhibited clinical signs consistent with DM but the histopathology was not typical for a diagnosis of DM [(Coates and Wininger 2010) and Figure 1]. Control tissue was obtained from age and breed matched unaffected dogs euthanized for causes unrelated to DM. Dogs were designated as controls if they had not exhibited clinical signs of DM and histological appearance of the thoracic spinal cord tissue was normal (Figure 1). See “Supplemental Information” for more details on sample collections.

Genotypes at canine *SOD1:c.118G>A* were determined using blood samples from each dog included in the study using a TaqMan^{TM} allelic discrimination assay that employed *5’-GTGGGCCTGTTGTGGTATCA-3’* with *5’-CAAACTGATGGACGTGGAATCC-3’* for the PCR primers and *5’-VIC-CTCGCCTTTAGTCAGC-MGB-3’* (*A* allele) and *5’-FAM-CGCCTTCAGTCAGC-MCB-3’* (*G* allele) for the completing probes (Awano et al. 2009).

DM-affected dogs were graded based on clinical signs at the time of euthanasia as described in Table I (Shelton et al. 2012). Confirmations of clinical diagnoses were made by evaluating sections of the thoracic spinal cords for the histopathological lesions that are characteristic of DM (March et al. 2009; Awano et al. 2009) (Figure 1). Diagnosis of DM was confirmed by observation of profound axonal loss, myelin loss, and marked astrogliosis in the dorsal portion of the lateral white matter in the thoracic spinal cord and by the presence of cytoplasmic aggregates in spinal cord motor neurons that bind anti-SOD1 antibodies (Figure 1) (Averill 1973; March et al. 2009; Awano et al. 2009). See

"Supplemental Information" for a detailed description of the methods employed for histopathological assessments. All of the dogs that were determined to be affected with DM based on clinical signs and cord histopathology contained aggregates in thoracic cord motor neurons that labeled with the SOD1 antibody. These SOD1-containing aggregates were not observed in the thoracic cord motor neurons of any of the dogs that had not exhibited any signs of DM at the time of euthanasia.

Myofiber type grouping and neuromuscular junction analysis

To determine whether DM was accompanied by changes in the distribution of fiber types in the intercostal muscles, sections of these muscles were immnolabeled with anti-myosin heavy chain type 1 (MHC-1) antibodies. This antibody selectively labels type 1 fibers. Detailed methods for immunolabeling are included in the Supplemental Materials section. Light microscopy was used to image the entire muscle cross section at a 100x magnification. Each composite image of a muscle section consisted of individual image frames stitched together. The frames were acquired by moving the specimen past the microscope objective in a raster pattern using an automated stage. Overlapping images of all areas of the section were captured in this manner and stitched into a composite image of the entire section by the Leica software. Proportions of type 1 fibers were calculated from individual frames using ImageJ^{TM} software. For each sample, two frames were randomly selected from each vertical pass of the stage during automated stitching (6-14 frames/sample section depending on size of the cross section). This method of sampling was used to acquire data representative of multiple fascicles within each muscle cross section.

The intercostal muscles were evaluated for contact between motor nerve terminals and the muscle acetylcholine receptor (AChR) complexes (Fischer et al. 2004). For these analyses, the AChR complexes were labeled with alpha bungarotoxin conjugated to AlexaFluor 594 (red fluorescence emission) and the nerve terminals were labeled with antineurofilament–light (NF-L) antibody localized with a secondary antibody conjugated to AlexaFluor 488 (green fluorescence emission. After the double-labeling, the preparations were examined with fluorescence microscopy to determine whether the nerve terminals made close contact with the AChR complexes. A detailed description of the methods used in these analyses is included in the Supplemental Materials section. At least 100 AChR complexes per sample were imaged, and these complexes were examined for the proximity of nerve terminals labeled with the anti-NF-L antibody. Images derived from the red and green channels were layered in PhotoShop, and transparency adjusted to assess the co-localization of labels. Neuromuscular junctions were scored as intact (continuous NF-L label overlapping with bungarotoxin label), partially intact (fragmented NF-L label adjacent to or co-localizing with bungarotoxin label), or absent (bungarotoxin label with no adjacent NF-L label) (Figure 7.A).

Morphometric analysis of myofibers

The intercostal muscles were evaluated for histopathology using paraffin sections labeled with hematoxylin and eosin (H&E) and Masson trichrome stains. Morphometric analyses were performed on these sections to assess for disease-related changes in muscle fiber size

and shape (Figure 2). A detailed description of the methods used in these analyses is provided in the Supplemental Materials section.

Statistical analyses

The data for Boxers and PWCs were analyzed independently. Data were analyzed for normality using a Shapiro-Wilk normality test. All data passed the normality test, thus Student's *t*-test was employed to compare affected and unaffected dogs.

RESULTS

SOD1 genotypes

Genotyping results for all dogs are summarized in table II. All DM-affected PWCs were homozygous for the A allele. Six unaffected PWCs had varying genotypes, including three that were homozygous for the A allele (Table II). All 5 DM-affected Boxers were homozygous for the A allele. Unaffected Boxers had varying genotypes, including one homozygous for the A allele (Table II). Of the unaffected PWCs homozygous for the A allele, all were 12 years and older at the time of euthanasia. The unaffected Boxer homozygous for the A allele was 9 years old when euthanized.

Intercostal muscle changes in late-stage DM dogs

Myofibers from unaffected PWCs and Boxers were generally uniform in size and shape (Figure 3), with some variability typical of old age (Braund et al. 1982). For both breeds, myofibers from early disease stage dogs were similar in appearance to those from controls (Figure 3. A). Severe atrophic changes were consistently seen in Grade 4 PWC muscle (Figure 3. C and D). Similar atrophy was occasionally seen in grade 3 PWC, but not in Grade 3 Boxers or in Grade 2 dogs from either breed. No Grade 4 Boxer intercostal muscles were available for this analysis. Collagen labeling was occasionally seen within myofiber fascicles of Grade 4 PWCs (Figure 3. D).

Increased variability in PWC intercostal myofiber size and shape

Individual myofibers were much more variable in size and shape in PWCs with end-stage DM than in age-matched unaffected dogs (Figure 4 and 5). Size histograms depict apparent differences in the distribution of the minor axis and area measures of fiber sizes of control and affected PWC myofibers (Figure 4. A and D). When data were divided into early and late disease groups (Figure 4. B and E), there was a larger percentage of myofibers with larger minor axis's in early stage, and a larger percentage of myofibers with smaller minor axis's in late stage PWC. There was no statistical significance between the mean myofiber minor axes or areas of control and affected PWCs. However, among PWCs there was a significantly larger range of myofiber sizes in the muscles from DM dogs compared to those from unaffected dogs (**minor axis length range**; control= 28.2 μm, affected = 43.4 μm: $p < 0.001$, **area range**; control =1,737 μm^2 affected= 2,8491 $\mu m^{2:}$ $p = 0.039$) (Figure 4. C and F). The percentage of angulated myofibers was on average larger in grade 4 PWC muscle than in unaffected PWCs (Control= 7.7% ± 3.5% (n= 6 dogs), affected = 14.5% ± 6.9% (n=4 dogs); p= 0.068). These data support the abnormal deviation from uniform fiber sizes

seen in figure 3.A, and coincide with the observation of abundant small atrophic fibers and large hypertrophic fibers in Grade 4 intercostal muscle.

Among Boxers, there were no significant differences in fiber size distributions between affected and unaffected dogs (Figure 5). However there was a peak in the medium-size range of both minor axis length and area parameters in early disease samples that was not present in the normal or late stage dogs (Figure 5 B and E).

Acetylcholine receptor (AChR) complexes remain innervated in DM affected intercostal muscle

Because atrophic myofibers are a prominent feature in late stage PWC intercostal muscle, we evaluated muscle AChR complexes to determine if they maintained close proximity with nerve terminals (Figure 6 A-C). No differences were seen between the percentages of intact, partially intact, or absent axons from affected and control dogs (Figure 6. D).

End stage intercostal muscles display shift to type 1 myofiber predominance

Unaffected and early stage Boxer and PWC muscles retained a normal checkerboard pattern of type 1 and type 2 fibers distributions (Figure 7. A). Late stage PWC samples displayed a dramatic shift to a predominance of type 1 fibers (Figure 7. B). The percentages of type 1 myofibers in an unaffected and grade 3 PWC samples were similar (Unaffected: 32%, grade 3, 39% and 38%). In two grade 4 PWCs, the percentage of myofibers that were of type 1 were 67% and 76%. Two Boxers, grade 2 and 3 had moderately higher proportions of type 1 myofibers (59% and 65%, respectively) than the one unaffected Boxer (49%). The control and Grade 3 Boxers had higher proportions of type 1 fibers compared to the PWCs with the same disease statuses. Only a limited number of samples suitable for these analyses were available because MHC-1 immunolabeling was hindered by formalin fixation.

DISCUSSION

Muscle atrophy is a classic and progressive feature in ALS patients and has also been reported in *SOD1* transgenic mouse models (Andersen et al. 1996; Charcot J-M 1869; Gurney et al. 1994; Wong et al. 1995). Our data indicate that this atrophy is recapitulated in the intercostal muscles in canine DM. The DM-related changes in muscle morphology are typical of those associated with denervation atrophy, suggesting neurogenic pathology due to altered motor neuron input to the muscle (Shelton et al. 2012). However there did not appear to be loss of physical contact of the motor nerve terminals with the intercostal muscle fibers. Among dogs with DM at the stages evaluated in this study, the disease is not accompanied by a loss of motor neurons from the thoracic cord or decreases in the numbers of motor axons in thoracic cord motor nerve (March et al. 2009). Therefore, if muscle atrophy was secondary to altered neural input, it appears that the cause must be primarily impaired motor neuron function without gross structural changes in the motor nerve terminals, axons or cell bodies. The finding that the neuromuscular junctions remain physically intact differs from findings in *SOD1* transgenic mouse models in which loss of contact between motor neuron terminal processes and muscle acetyl choline receptor

complexes has been reported (Dadon-Nachum et al. 2011; Fischer et al. 2013; Fischer et al. 2004; Frey et al. 2000; Schaefer et al. 2005).

In a recent study, electrodiagnostic evaluations of dogs with DM indicated functional impairment of pelvic limb muscles in early disease stages when dogs become nonambulatory, whereas histopathological evidence of denervation was not apparent until advanced disease stages (Shelton et al. 2012). Similar findings have been described in some ALS and Charcot-Marie-Tooth mouse models where abnormal motor function and muscle pathology existed without significant physical evidence of denervation (Lobsiger et al. 2005; Shen et al. 2011). In ALS patients, electrodiagnostic evaluation of diaphragm and intercostal muscles revealed fibrillation sharp waves, indicative of denervation, which correlated with respiratory muscle weakness (de Carvalho et al. 2010). Whether there is a similar physical preservation of the neuromuscular junctions in human ALS intercostal muscles remains to be determined. This will be important to evaluate with respect to further assessing both DM and *SOD1* transgenic mice as models for ALS.

In comparing pathological changes associated with DM or ALS, it is important to note that similar changes may occur at different stages of the disease in different muscle groups and in the nerves associated with these muscles, Weakness and atrophy of limb muscles are relatively early to mid-stage signs of both ALS and DM, whereas respiratory impairment is a relatively late manifestation of these diseases. Therefore, the intercostal muscles evaluated in this study most likely represent the earlier phase of the degenerative process and therefore provide information on a different stage of the pathogenesis than the hind limb muscles obtained at the same disease stages (Shelton et al. 2012). Likewise, the fibular nerve pathology reported in DM (Shelton et al. 2012) may be more advanced at the same disease stage than any pathology that might be present in nerves associated with the intercostal muscles.

It has been widely reported that neurogenic atrophy in muscle from ALS patients is accompanied by fiber-type grouping, postulated to occur when denervated myofibers are reinnervated by collateral sprouts from neighboring axons (Andersen et al. 1996; Fischer et al. 2004; Schaefer et al. 2005; Soraru et al. 2008). On the other hand, it has also been reported that muscle biopsies from ALS patients exhibit muscle fiber atrophy but no fiber type grouping (Baloh et al. 2007). The reason for this apparent discrepancy is not apparent from the data available, but ALS actually encompasses a spectrum of disorders, and it is possible that fiber type grouping occurs in some forms of the disease and not others (Soraru et al. 2008). Because no type grouping in intercostal muscle (this study) or in pelvic limb muscles (Shelton et al. 2012), has been identified in PWCs with late stage DM, it appears that this breed recapitulates muscle pathology of only some forms of ALS. The pronounced increase in the ratio of type 1 to type 2 fibers seen in end stage PWCs, relative to that in a normal PWC, has also been reported in hind limb muscle from an ALS mouse model with a low copy number of a mutant *SOD1* transgene (Acevedo-Arozena et al. 2011). This change could result from fiber-type switching without changes in neural input (Bassel-Duby and Olson 2006; Simmons et al. 2011). Alternatively, DM may result in a preferential loss of type 2 fibers. In ALS mouse models, myofibers expressing the type 1 myosin isoform are more resistant to disease (Acevedo-Arozena et al. 2011; Frey et al. 2000; Hegedus et al.

2007). This could also be the case for the intercostal muscles in DM and in at least some forms of ALS.

Although the fiber type composition was evaluated in a limited number of dogs in the present study, it appears that there may be significant breed differences in distribution of fiber types in the intercostal muscles (Armstrong et al. 1982). Thus, for evaluation of disease progression in DM, it appears that data from different breeds should not be pooled. Because PWCs tend to be euthanized at all stages of the disease process whereas very few Boxers are maintained until disease end stage, it would be more practical to focus future studies on the PWC breed as a disease model.

In DM histopathology, both in the intercostal muscles and in pelvic limb muscles, occurs late in the disease process (Shelton et al. 2012), suggesting that DM may be a very useful model for studying the mechanisms underlying the development of muscle pathology in ALS. Tissue samples available from ALS patients, particularly nervous tissues, have primarily been collected postmortem from patients who died as a consequence of the disease and not prior to the development of advanced histopathology. On the other hand, tissue samples can be collected from PWCs at all stages of DM disease progression. Larger breed (Boxers) dogs are usually euthanized when nonambulatory paraparesis develops so tissues representing late stage disease are difficult to obtain from this or other larger breed with DM. Functional and biochemical analyses of early stage muscle and nerve is likely to provide insight into the process that culminates in the types of late-stage muscle histopathology characteristic of both DM and ALS.

In this study, we found that not all dogs homozygous for the *SOD1* mutation develop DM and none of the dogs that were heterozygous for this mutation developed the disease. In a cohort of 239 dogs of multiple breeds that were homozygous for the A allele and over 9 years of age, 25 had not exhibited signs of DM (unpublished data). This is consistent with a previous report that this *SOD1* mutation in DM is associated with an incompletely penetrant autosomal recessive mode of inheritance (Awano et al. 2009). Similarly, it has also been reported that the *D90A- SOD1* mutation in ALS patients can be inherited in an autosomal recessive and incompletely penetrant pattern (Al-Chalabi et al. 1998; Andersen et al. 1996; Andersen et al. 1995; Khoris et al. 2000). Patients with the adult onset recessive form of ALS are speculated to have also inherited a protective modifier, tightly linked with *SOD1*, from a common ancestor (Al-Chalabi et al. 1998). This hypothetical modifier is proposed to decrease the toxicity of the mutant allele so that two copies are required to produce an ALS phenotype. The existence of a hypothetical modifier similar to that which has been proposed for ALS could also explain why some dogs that are homozygous for the *SOD1:c.118G>A* mutation fail to develop DM, even at advanced ages. Determining why some dogs that are homozygous for the *SOD1* mutation fail to develop DM may provide clues on how to prevent or delay the development and progression of DM in dogs and ALS in people with predisposing *SOD1* mutations.

Overall these studies indicate that DM will be a very useful model in elucidating the mechanisms underlying neuromuscular pathology in at least some forms of ALS. The muscle pathology in the canine disease recapitulates that which occurs in the human

disorder. The ability to obtain tissues from affected dogs in the early stages of the disease process will enable characterization of the pathogenesis of disease progression that is not possible with ALS. DM is also likely to be a good disease model for evaluating potential therapeutic interventions for some forms of ALS.

Acknowledgments

We thank Aleksandr Jurkevic for technical support, Dr. Diane Shelton and Dr. Michael Garcia for helpful advice, and Cheryl Jensen for participating as a masked evaluator. Tissue collections were generously performed by Drs. Eugene Garcia, Sydney Moise, Scott Loxley, Bethany Russell, Davinne Glenn, Scott Driever, Daniel Hartney, Gary Volk, Carley Giovanella, Gary Volk, Chris Roth, Ben Moody, Dawn Mehra, Thomas Wolski, Robert Kroll, Dr. Chad Westbrook, Shelley Newman, Lynn Johnson, Rebecca Tremble, Robert Slobody, Tammy Stevenson, and Brenda Perkins.

This work was supported by the AKC Canine Health Foundation, ALS Association, a Phi Zeta Research Award, an Ada Mae Clough Scholarship (to ACB), a University of Missouri Research Council grant, and the U.S. Department of Education's Graduate Assistance in Areas of National Need (GAANN) program.

References

Acevedo-Arozena A, Kalmar B, Essa S, Ricketts T, Joyce P, Kent R, Rowe C, Parker A, Gray A, Hafezparast M, Thorpe JR, Greensmith L, Fisher EM. A comprehensive assessment of the SOD1G93A low-copy transgenic mouse, which models human amyotrophic lateral sclerosis. Disease models & mechanisms. 2011; 4(5):686–700. [PubMed: 21540242]

Al-Chalabi A, Andersen PM, Chioza B, Shaw C, Sham PC, Robberecht W, Matthijs G, Camu W, Marklund SL, Forsgren L, Rouleau G, Laing NG, Hurse PV, Siddique T, Leigh PN, Powell JF. Recessive amyotrophic lateral sclerosis families with the D90A SOD1 mutation share a common founder: evidence for a linked protective factor. Hum Mol Genet. 1998; 7(13):2045–2050. [PubMed: 9817920]

Al-Chalabi A, Jones A, Troakes C, King A, Al-Sarraj S, van den Berg LH. The genetics and neuropathology of amyotrophic lateral sclerosis. Acta Neuropathol. 2012; 124(3):339–352. [PubMed: 22903397]

Andersen PM, Forsgren L, Binzer M, Nilsson P, Ala-Hurula V, Keranen ML, Bergmark L, Saarinen A, Haltia T, Tarvainen I, Kinnunen E, Udd B, Marklund SL. Autosomal recessive adult-onset amyotrophic lateral sclerosis associated with homozygosity for Asp90Ala CuZn-superoxide dismutase mutation. A clinical and genealogical study of 36 patients. Brain. 1996; 119(Pt 4):1153–1172. [PubMed: 8813280]

Andersen PM, Nilsson P, Ala-Hurula V, Keranen ML, Tarvainen I, Haltia T, Nilsson L, Binzer M, Forsgren L, Marklund SL. Amyotrophic lateral sclerosis associated with homozygosity for an Asp90Ala mutation in CuZn-superoxide dismutase. Nat Genet. 1995; 10(1):61–66. [PubMed: 7647793]

Armstrong RB, Saubert CWt, Seeherman HJ, Taylor CR. Distribution of fiber types in locomotory muscles of dogs. Am J Anat. 1982; 163(1):87–98. [PubMed: 6460435]

Averill DR Jr. Degenerative myelopathy in the aging German Shepherd dog: clinical and pathologic findings. J Am Vet Med Assoc. 1973; 162(12):1045–1051. [PubMed: 4196853]

Awano T, Johnson GS, Wade CM, Katz ML, Johnson GC, Taylor JF, Perloski M, Biagi T, Baranowska I, Long S, March PA, Olby NJ, Shelton GD, Khan S, O'Brien DP, Lindblad-Toh K, Coates JR. Genome-wide association analysis reveals a SOD1 mutation in canine degenerative myelopathy that resembles amyotrophic lateral sclerosis. Proc Natl Acad Sci U S A. 2009; 106(8): 2794–2799. [PubMed: 19188595]

Baloh RH, Rakowicz W, Gardner R, Pestronk A. Frequent atrophic groups with mixed-type myofibers is distinctive to motor neuron syndromes. Muscle Nerve. 2007; 36(1):107–110. [PubMed: 17299742]

Bassel-Duby R, Olson EN. Signaling pathways in skeletal muscle remodeling. Annu Rev Biochem. 2006; 75:19–37. [PubMed: 16756483]

Braund KG, McGuire JA, Lincoln CE. Observations on normal skeletal muscle of mature dogs: a cytochemical, histochemical, and morphometric study. Vet Pathol. 1982; 19(6):577–595. [PubMed: 7147621]

Brooks BR, Miller RG, Swash M, Munsat TL. El Escorial revisited: revised criteria for the diagnosis of amyotrophic lateral sclerosis. Amyotroph Lateral Scler Other Motor Neuron Disord. 2000; 1(5): 293–299. [PubMed: 11464847]

Charcot J-M JA. Deuxcas d'atrophie musculaire progressive avec lesions del substance grise et de faisceaux anterolateraux de moelle epiniere. Arch Phusiol Norm Pathol. 1869:354–357.

Coates JR, March PA, Oglesbee M, Ruaux CG, Olby NJ, Berghaus RD, O'Brien DP, Keating JH, Johnson GS, Williams DA. Clinical characterization of a familial degenerative myelopathy in Pembroke Welsh Corgi dogs. J Vet Intern Med. 2007; 21(6):1323–1331. [PubMed: 18196743]

Coates JR, Wininger FA. Canine degenerative myelopathy. Vet Clin North Am Small Anim Pract. 2010; 40(5):929–950. [PubMed: 20732599]

Dadon-Nachum M, Melamed E, Offen D. The “dying-back” phenomenon of motor neurons in ALS. J Mol Neurosci. 2011; 43(3):470–477. [PubMed: 21057983]

de Carvalho M, Pinto S, Swash M. Association of paraspinal and diaphragm denervation in ALS. Amyotroph Lateral Scler. 2010; 11(1-2):63–66. [PubMed: 19533450]

Fischer LR, Brotherton T, Glass JD. Axonal degeneration in the peripheral nervous system: Implications for the pathogenesis of amyotrophic lateral sclerosis. Exp Neurol. 2013

Fischer LR, Culver DG, Tennant P, Davis AA, Wang M, Castellano-Sanchez A, Khan J, Polak MA, Glass JD. Amyotrophic lateral sclerosis is a distal axonopathy: evidence in mice and man. Exp Neurol. 2004; 185(2):232–240. [PubMed: 14736504]

Frey D, Schneider C, Xu L, Borg J, Spooren W, Caroni P. Early and selective loss of neuromuscular synapse subtypes with low sprouting competence in motoneuron diseases. J Neurosci. 2000; 20(7): 2534–2542. [PubMed: 10729333]

Griffiths IR, Duncan ID. Chronic degenerative radiculomyelopathy in the dog. J Small Anim Pract. 1975; 16(8):461–471. [PubMed: 1195675]

Gurney ME, Pu H, Chiu AY, Dal Canto MC, Polchow CY, Alexander DD, Caliendo J, Hentati A, Kwon YW, Deng HX, et al. Motor neuron degeneration in mice that express a human Cu,Zn superoxide dismutase mutation. Science. 1994; 264(5166):1772–1775. [PubMed: 8209258]

Hegedus J, Putman CT, Gordon T. Time course of preferential motor unit loss in the SOD1 G93A mouse model of amyotrophic lateral sclerosis. Neurobiol Dis. 2007; 28(2):154–164. [PubMed: 17766128]

Khoris J, Moulard B, Briolotti V, Hayer M, Durieux A, Clavelou P, Malafosse A, Rouleau GA, Camu W. Coexistence of dominant and recessive familial amyotrophic lateral sclerosis with the D90A Cu,Zn superoxide dismutase mutation within the same country. Eur J Neurol. 2000; 7(2):207–211. [PubMed: 10809943]

Lobsiger CS, Garcia ML, Ward CM, Cleveland DW. Altered axonal architecture by removal of the heavily phosphorylated neurofilament tail domains strongly slows superoxide dismutase 1 mutant-mediated ALS. Proc Natl Acad Sci U S A. 2005; 102(29):10351–10356. [PubMed: 16002469]

March PA, Coates JR, Abyad RJ, Williams DA, O'Brien DP, Olby NJ, Keating JH, Oglesbee M. Degenerative myelopathy in 18 Pembroke Welsh Corgi dogs. Vet Pathol. 2009; 46(2):241–250. [PubMed: 19261635]

Rosen DR, Siddique T, Patterson D, Figlewicz DA, Sapp P, Hentati A, Donaldson D, Goto J, O'Regan JP, Deng HX, et al. Mutations in Cu/Zn superoxide dismutase gene are associated with familial amyotrophic lateral sclerosis. Nature. 1993; 362(6415):59–62. [PubMed: 8446170]

Schaefer AM, Sanes JR, Lichtman JW. A compensatory subpopulation of motor neurons in a mouse model of amyotrophic lateral sclerosis. J Comp Neurol. 2005; 490(3):209–219. [PubMed: 16082680]

Shelton GD, Johnson GC, O'Brien DP, Katz ML, Pesayco JP, Chang BJ, Mizisin AP, Coates JR. Degenerative myelopathy associated with a missense mutation in the superoxide dismutase 1 (SOD1) gene progresses to peripheral neuropathy in Pembroke Welsh Corgis and Boxers. J Neurol Sci. 2012; 318(1-2):55–64. [PubMed: 22542607]

Shen H, Barry DM, Dale JM, Garcia VB, Calcutt NA, Garcia ML. Muscle pathology without severe nerve pathology in a new mouse model of Charcot-Marie-Tooth disease type 2E. Hum Mol Genet. 2011; 20(13):2535–2548. [PubMed: 21493625]

Simmons BJ, Cohen TJ, Bedlack R, Yao TP. HDACs in skeletal muscle remodeling and neuromuscular disease. Handb Exp Pharmacol. 2011; 206:79–101. [PubMed: 21879447]

Soraru G, D'Ascenzo C, Nicolao P, Volpe M, Martignago S, Palmieri A, Romeo V, Koutsikos K, Piccione F, Cima V, Pegoraro E, Angelini C. Muscle histopathology in upper motor neuron-dominant amyotrophic lateral sclerosis. Amyotrophic Lateral Sclerosis. 2008; 9(5):287–293. [PubMed: 18608096]

Victor Dubowitz, CAS. Muscle Biopsy: A Practical Approach. Saunders Elsevier; 2007.

Wininger FA, Zeng R, Johnson GS, Katz ML, Johnson GC, Bush WW, Jarboe JM, Coates JR. Degenerative Myelopathy in a Bernese Mountain Dog with a Novel SOD1 Missense Mutation. J Vet Intern Med. 2011; 25(5):1166–1170. [PubMed: 21848967]

Wong PC, Pardo CA, Borchelt DR, Lee MK, Copeland NG, Jenkins NA, Sisodia SS, Cleveland DW, Price DL. An adverse property of a familial ALS-linked SOD1 mutation causes motor neuron disease characterized by vacuolar degeneration of mitochondria. Neuron. 1995; 14(6):1105–1116. [PubMed: 7605627]

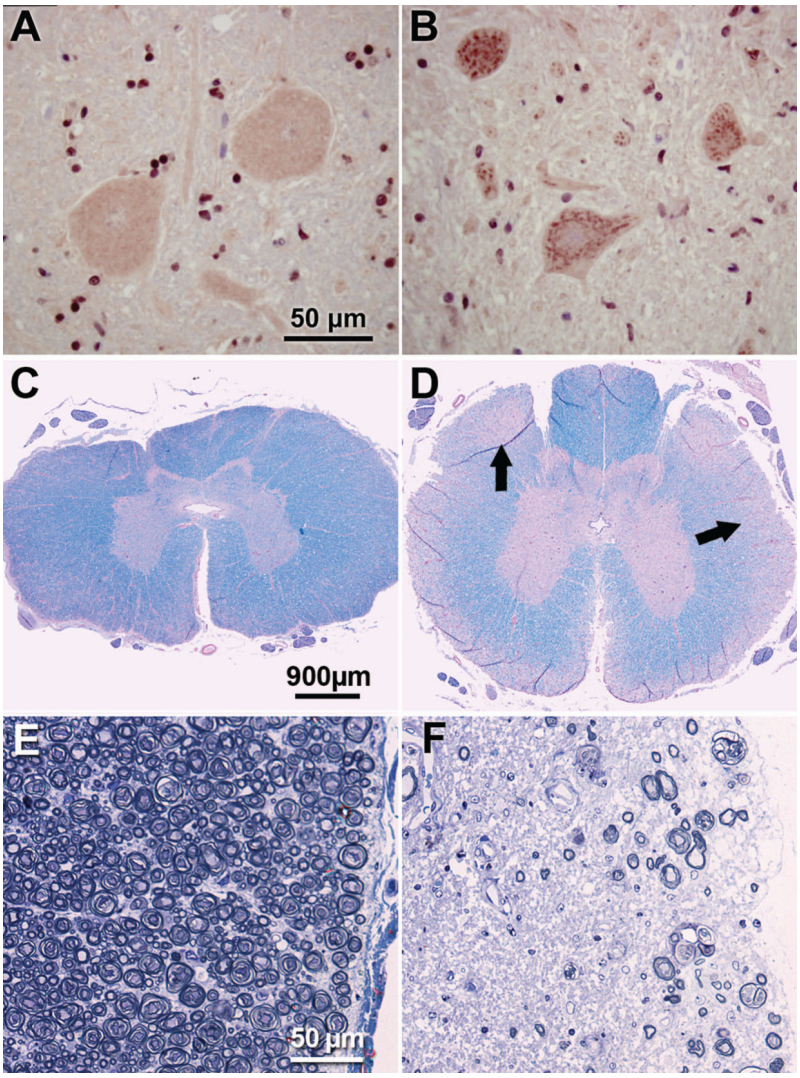

Figure 1. DM-affected spinal cords display SOD1-positive aggregates in motor neurons and marked myelinated axon loss in white matter

Immunohistochemical demonstration of SOD1-containing aggregates in motor neurons in the thoracic spinal cord (A,B). Numerous aggregates stained with an antibody directed against SOD1 were present in ventral horn motor neurons from a DM-affected PWC (B). Similar aggregates were present in all affected dogs of both PCW and Boxer breeds. These inclusions were not observed in thoracic cord motor neurons from unaffected dogs (representative preparation from a control PWC shown in B). Luxol fast blue and periodic acid-Schiff stained thoracic spinal cord from unaffected (C) and grade 4 (D) PWCs. Pallor of the peripheral white matter in (D) corresponds to axonal loss and demyelination (arrows). Higher magnification of thoracic white matter from unaffected (E) and grade 4 (F) PWCs stained with toluidine-blue. Substantial axonal loss with myelin pathology is seen in the PWC with advanced DM. Bars in (A), (C) and (E) indicate magnifications in (B), (D) and (F) respectively.

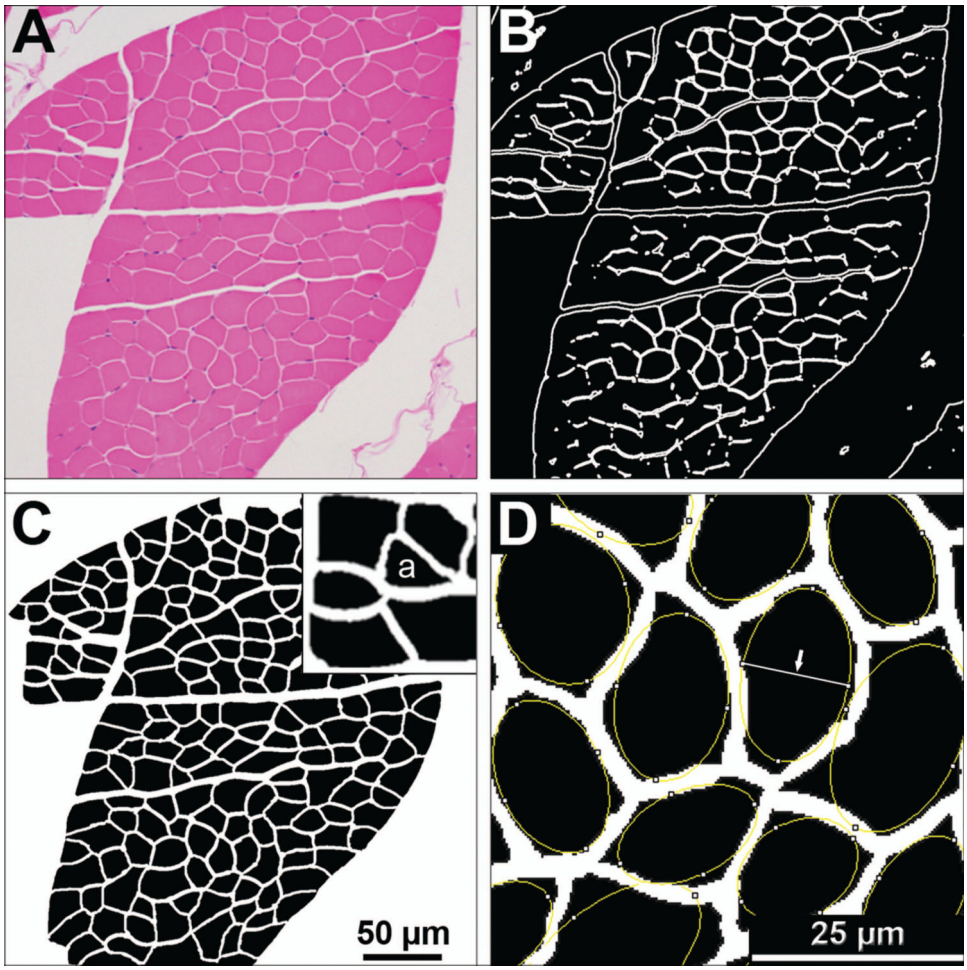

Figure 2. Method for morphometric analysis of myofibers

(A) Hematoxylin and eosin stained intercostal muscle cross sections were imaged with light microcopy at a 200x magnification. (B) Fiji^{TM} or Photoshop^{TM} imaging software were used to generate a black and white segmented mask outlining the boundaries of each myofiber. (C) In Photoshop^{TM}, the mask was overlaid on the gray-scaled original image, transparency increased, and manual corrections were made to define the boundaries of each fiber. Once boundaries are defined, the corrected mask is thresholded in Fiji^{TM}, and a particle analysis tool was used to obtain measurements. Measurements include minor axis length, fiber cross sectional area, and roundness. (D) The minor axis is identified as the shortest axis of a best fit ellipse (Arrow). Pixels of this axis and of the cross sectional areas were converted to µm and µm^2 respectively for each myofiber. The percent of angulated fibers (example labeled with “a” in insert of panel C) were determined manually by a masked evaluator.

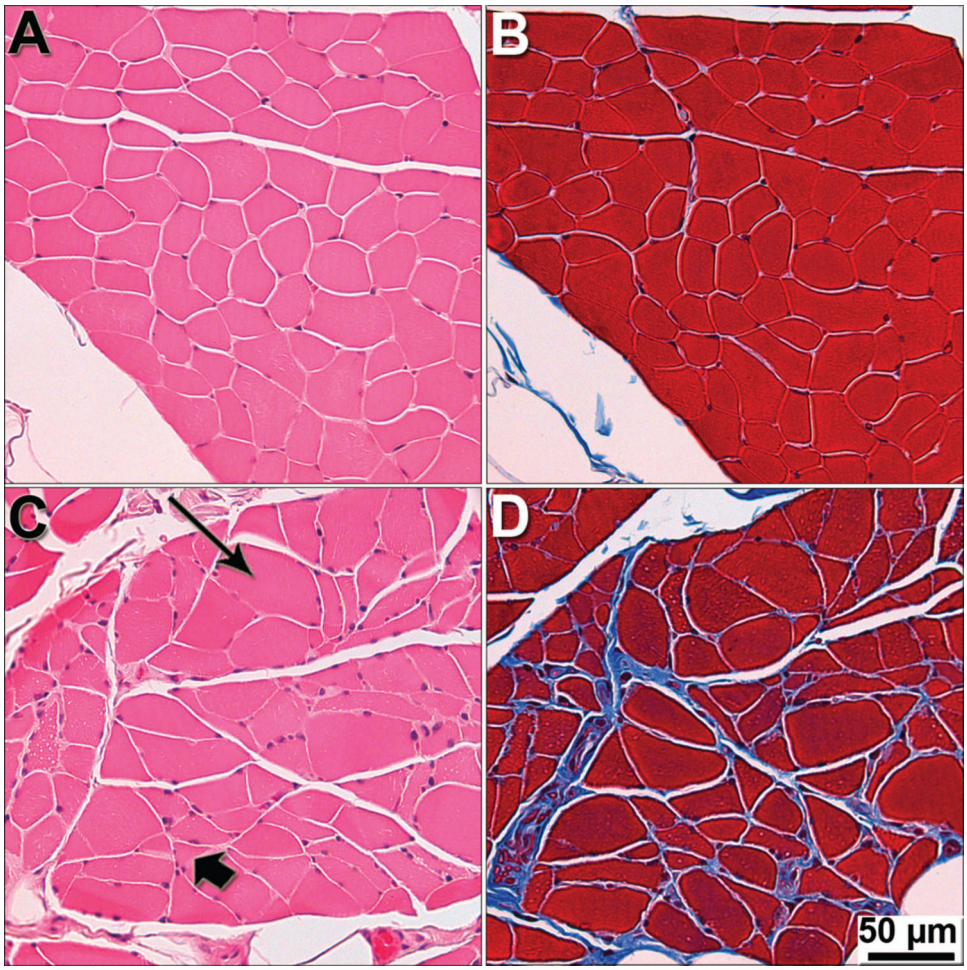

Figure 3. Severe pathology in intercostal muscle of end-stage DM dogs

Intercostal muscles were stained with H&E (A and C), and Masson trichrome (B and D), to visualize general morphology of myofibers and presence of fibrotic tissue. (A and B) Myofibers from a control PWC display uniform size and shape with no fibrosis seen between fibers. (C) Myofibers from a grade 4 PWC showing variability in size and shape with hypertrophy (long arrow) and atrophy (short arrow) fibers. (D) End-stage PWC displaying fibrosis (blue stain).

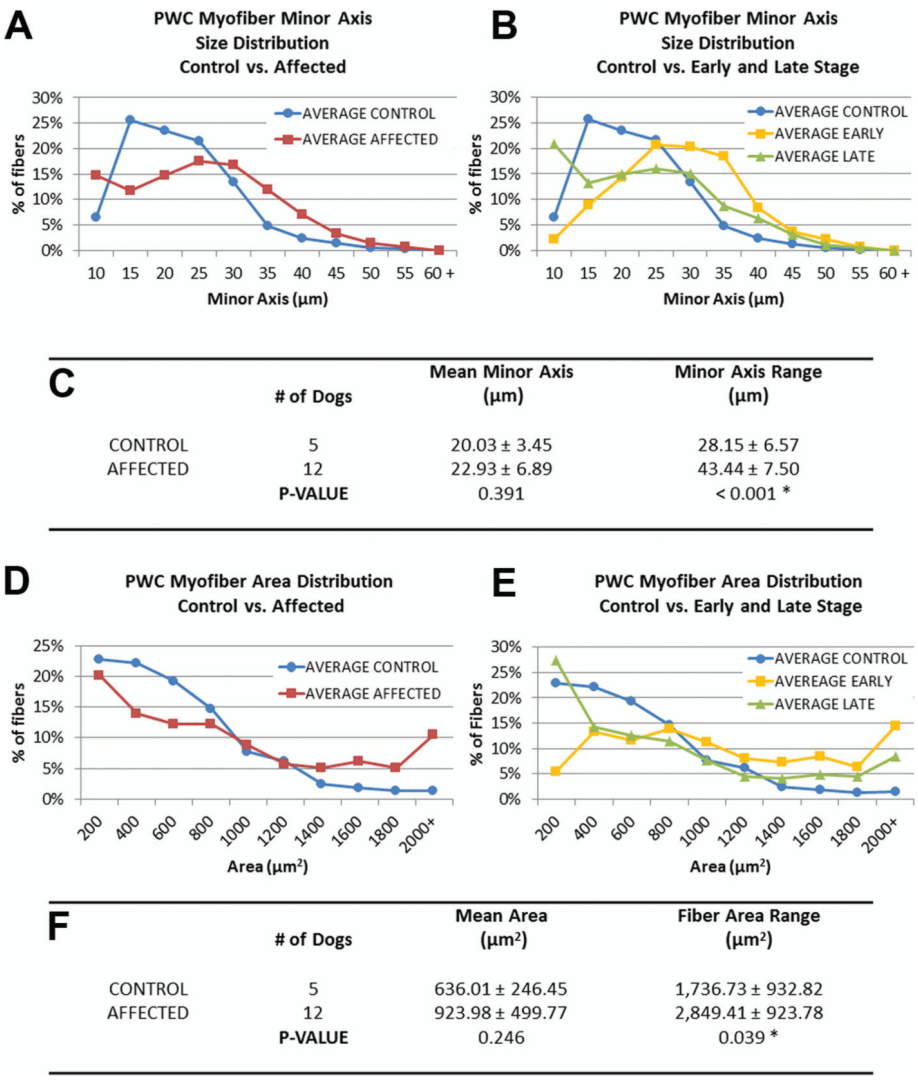

Figure 4. Morphometric data reveal increased variability of intercostal myofiber sizes in DM-affected PWCs

(A, D) Size distribution graphs of myofibers from affected PWCs show changes in the distribution of fibers sizes (minor axis, and cross sectional area respectively). (B, E) Distribution graph of affected PWCs separated into early (n = 3) and late (n=9) stages. Early stage myofiber distributions were shifted towards larger size classes, while more small fibers were seen in the late stage distribution. (C, F) No significant difference was seen between the mean minor axis lengths or cross sectional area of unaffected and affected dogs; however the range of fiber sizes were significantly increased in affected PWCs (* $p<0.05$).

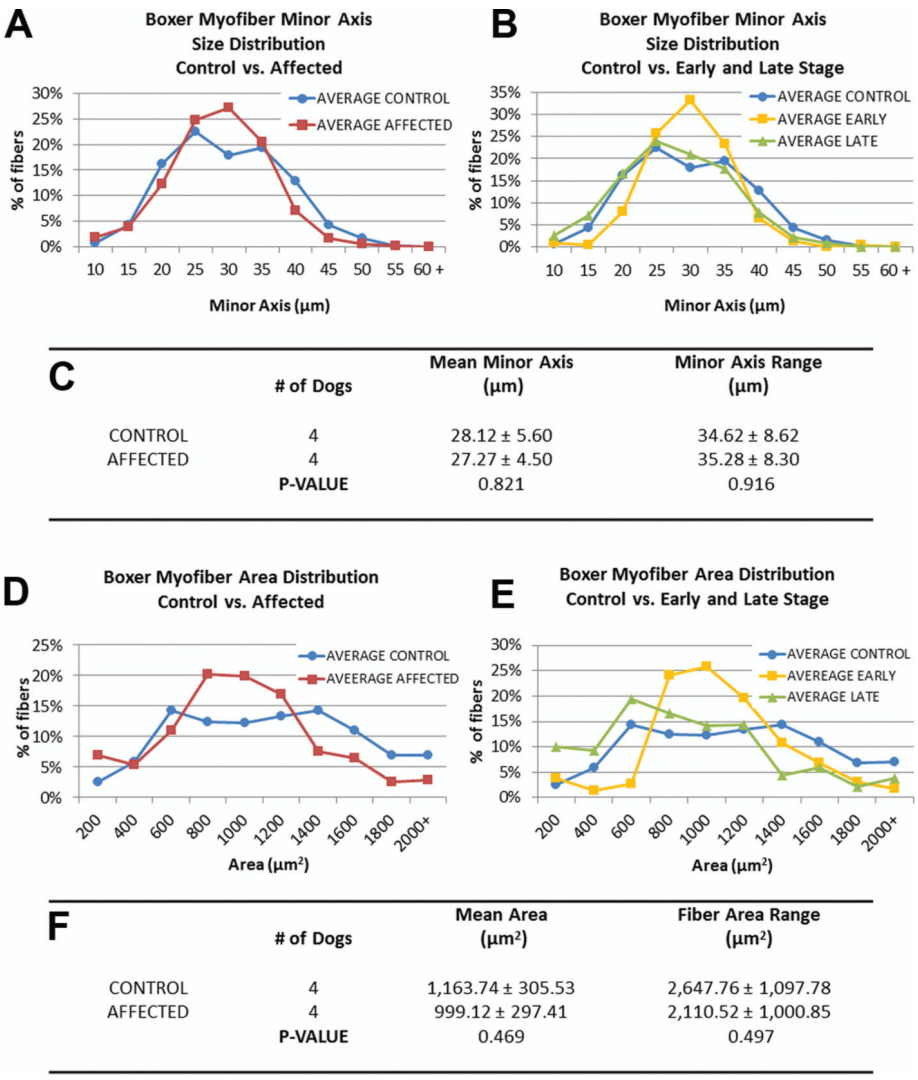

Figure 5. Boxer morphometric data reveal no significant differences in intercostal myofiber sizes

(A, D) Size distributions of minor axis length and cross-sectional area of myofibers from unaffected and affected samples. (B, E) When affected dog data is separated into early and late stage (early: n=2, Late: n=2), early disease samples exhibit a peak in the medium size range. (C, F) No significant differences were detected in mean minor axis length or range between control and affected groups.

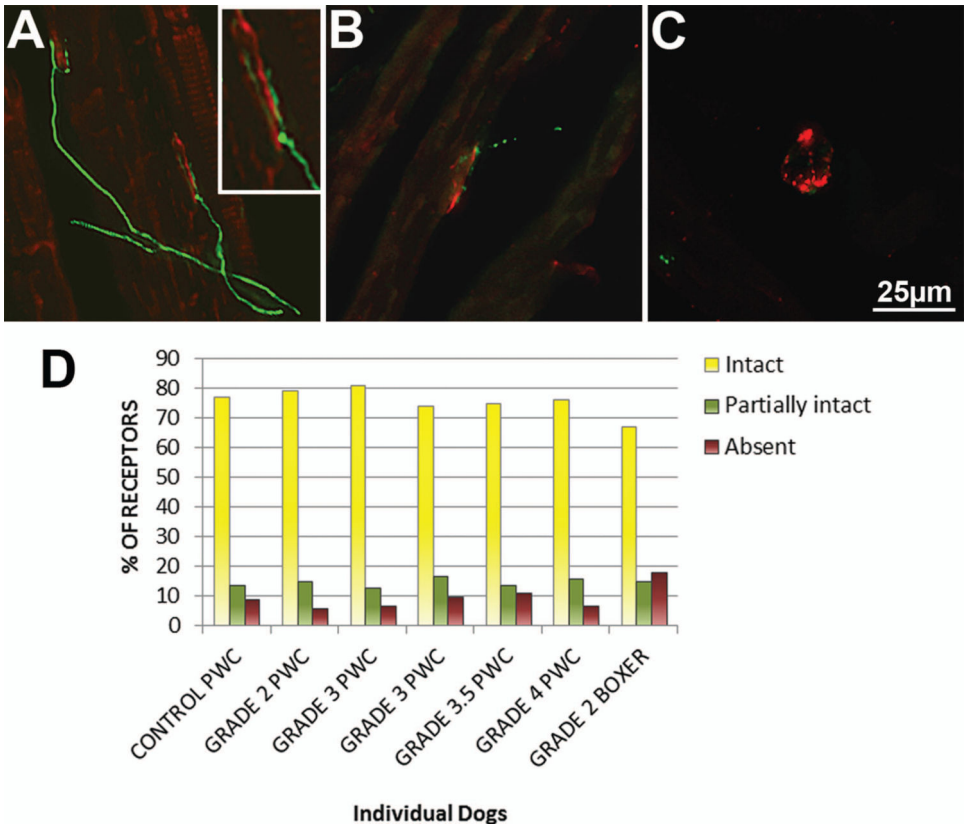

Figure 6. Acetylcholine receptor (AChR) complexes remain innervated in DM affected intercostal muscle

Thoracic intercostal muscle from one unaffected and six affected dogs were stained with alpha bungarotoxin to label AChR's (red), and anti-NF-L to label axon terminals (green). At least 100 complexes were imaged from each sample. Axons were scored based on proximity to AChR complexes as intact (A), partially intact (B), or absent (C). (D) Bar graph showing the percentage of receptors from each sample that were intact, partially intact, or absent. Insert in A is a higher magnification showing contact between the nerve terminal and the receptor complex. A-C are representative images of observations from control and affected samples.

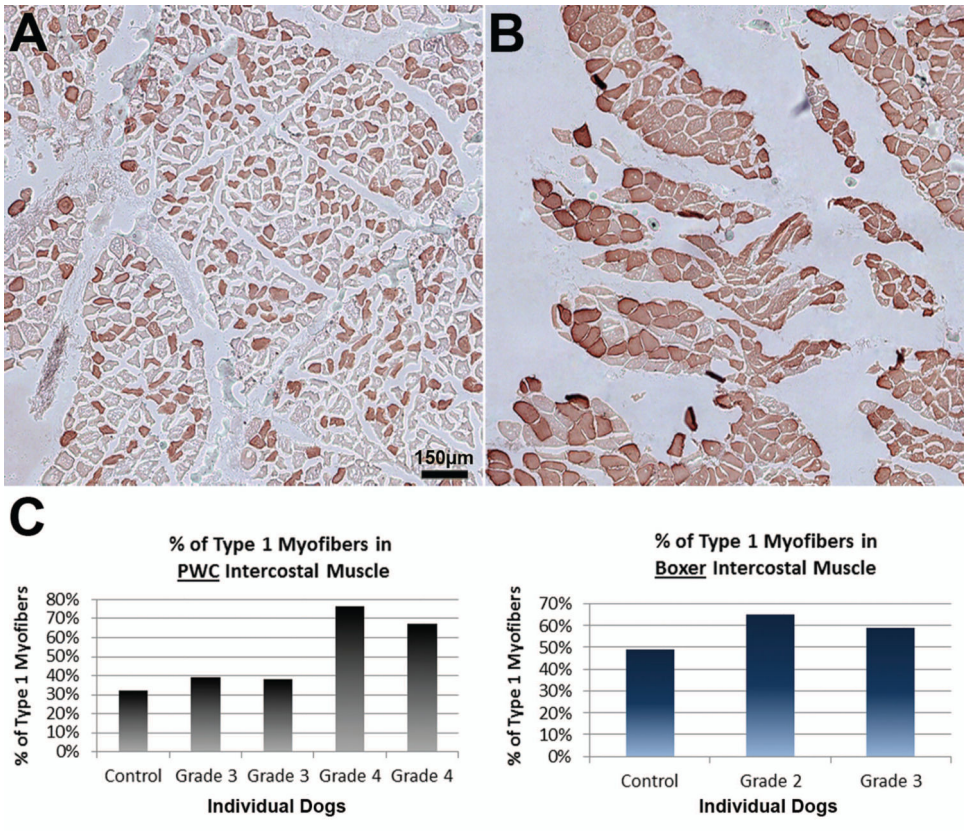

Figure 7. Changes in fiber type patterns in intercostal muscle of end stage DM dogs

Intercostal muscles were stained with anti-myosin heavy chain-1 to visualize the proportions of fiber types. (A) Unaffected PWC with normal checkerboard pattern of type 1 and 2 fibers. (B) Grade 4 PWC with a high predominance of type 1 fibers. Bar in (A) represents magnification in both images. (C) Bar graph displaying % of type 1 myofibers in PWC (left) and Boxer (right) thoracic intercostal muscle. PWC graph correlates with observations, with a larger percentage of type 1 fibers in grade 4 dogs (control n = 1, affected n = 4). (Boxers: control n= 1, affected n =2).

Table 1

Clinical grading scale of disease progression in DM affected dogs.

Clinical Grade	Clinical Signs[a]
1	**Paraparesis and General Proprioceptive Ataxia** •Progressive general proprioceptive ataxia •Asymmetric and spastic paraparesis •Postural reaction deficits in pelvic limb •Intact spinal reflexes (patellar reflex may be decreased)
2	**Nonambulatory Paraparesis to Paraplegia** •Mild to moderate loss of muscle mass in pelvic limbs •Reduced to absent spinal reflexes in pelvic limbs •+/- urinary and fecal incontinence
3	**Paraplegia to Thoracic Limb Weakness** •Signs of thoracic limb weakness •Flaccid paraplegia •Absence of spinal reflexes in pelvic limbs •Severe loss of muscle mass in pelvic limbs •Urinary and fecal incontinence
4	**Tetraplegia and Brain Stem Signs** •Flaccid tetraplegia •Difficulty with swallowing and tongue movements •Absence of spinal reflexes in all limbs •Reduced to absent cutaneous trunci reflex •Generalized and severe loss of muscle mass •Urinary and fecal incontinence

[a]The presumptive diagnosis of DM for dogs was based on the presence and progression of these signs. Early stages include grades 1-2, and late stages include grades 3-4. (Adapted from Coates and Wininger 2010; Shelton et al 2012)

Table II

SOD1 Genotypes

	Number of Dogs of Each *SOD1* Genotype (age in years)		
Disease Status - Breed	G/G	A/G	A/A
Unaffected PWC	1 (16)	2 (14, 17)	3 (12 to 14)
Affected PWC	0	0	14 (12 to 15)
Unaffected Boxer	1 (8)	2 (12, 13)	1 (9)
Affected Boxer	0	0	5 (9 to 12)